Invited Article: Optical trapping of ultrasmooth gold nanoparticles in liquid and air

Y. Arita, G. Tkachenko, N. McReynolds, N. Marro, W. Edwards, E. R. Kay, and K. Dholakia

Invited Article: Optical trapping of ultrasmooth gold nanoparticles in liquid and air

Y. Arita,[1,2,a] G. Tkachenko,[1] N. McReynolds,[1] N. Marro,[3] W. Edwards,[3] E. R. Kay,[3] and K. Dholakia[1,4,b]

[1]*SUPA, School of Physics and Astronomy, University of St Andrews, North Haugh, Fife KY16 9SS, United Kingdom*
[2]*Molecular Chirality Research Center, Chiba University, 1-33 Yayoi-cho, Inage-ku, Chiba-shi 263-0022, Japan*
[3]*EaStCHEM, School of Chemistry, University of St Andrews, North Haugh, Fife KY16 9ST, United Kingdom*
[4]*Graduate School of Engineering, Chiba University, 1-33 Yayoi-cho, Inage-ku, Chiba-shi 263-0022, Japan*

Optical manipulation of gold nanoparticles has emerged as an exciting avenue for studies in nanothermometry, cell poration, optical binding, and optomechanics. However, conventional gold nanoparticles usually depart from a spherical shape, making such studies less controlled and leading to potential artifacts in trapping behavior. We synthesize ultrasmooth gold nanoparticles, which offer improved circularity and monodispersity. In this article, we demonstrate the advantages of such nanoparticles through a series of optical trapping experiments in both liquid and air. Compared to their conventional counterparts, ultrasmooth gold nanoparticles exhibit up to a two-fold and ten-fold reduction in standard deviation for trap stiffness measurements in liquid and air, respectively. They will enable more controlled studies of plasmon mediated light-matter interactions. *© 2018 Author(s). All article content, except where otherwise noted, is licensed under a Creative Commons Attribution (CC BY) license (http://creativecommons.org/licenses/by/4.0/).* https://doi.org/10.1063/1.5030404

I. INTRODUCTION

Optical manipulation of mesoscopic particles has facilitated a wide range of innovative science and applications. Though the majority of studies have focused upon the use of micron sized dielectric objects, in 1994 it was established by Svoboda and Block that gold nanoparticles (NPs) of sizes below 100 nm could readily be trapped.[1] Trapping at this size scale is perhaps surprising at first given the cubic dependency of the polarizability (and thus the optical gradient force) on the particle size for dielectric particles. The trapping behavior is explained by gold's large polarizability leading to very strong optical gradient forces and three-dimensional trapping[2–4] for such small particles.

Subsequent investigations have shown a vast array of fascinating studies using gold NPs, with many exploiting the surface plasmon resonance, thus leading to a strong wavelength dependence of their trapping behavior.[5–7] Notably, the chemical properties of gold lead to routes for custom functionalization for biomedically relevant applications. Very recently, a suite of studies have come to the fore exploring the trapping of gold NPs for optical binding,[8] trapping in air,[9] and other studies including their potential use as local heaters or handles in biological investigations.[4] Moreover, laser-induced breakdown of gold NPs can be used for cell poration.[10]

In virtually all investigations, gold NPs have been sourced commercially and an inherent aspect of their response has been due to their morphology. For example, in a key study in 2005, gold NPs were seen to exhibit unexpected trapping characteristics, as particles as large as 254 nm could be stably

---

[a]Electronic mail: ya10@st-andrews.ac.uk
[b]Electronic mail: kd1@st-andrews.ac.uk

trapped in three-dimensional potential well by a single beam.[2] This experimental result was revisited by a recent study including a theoretical model based on the coupled dipole method.[11] The model suggests that particles larger than 170 nm can be stably trapped only if they deviate from a perfect spherical shape, which is commonly assumed for gold NPs. Indeed, scanning electron microscopy has revealed that commercially available gold NPs are inherently non-spherical and rather appear in the shape of icosahedron, decahedron, triangular, or hexagonal prism structures.[11,12] The morphological features of such particles are responsible for their orientation with respect to the beam polarization, which enhances their trap stiffness. A step forward would be to avoid such non-uniformity in shape to enable more reproducible studies, including consideration of heating with gold NPs for a wide range of trapping experiments.

In this article, we synthesize ultrasmooth (US) monocrystalline gold NPs and compare them with conventional gold NPs, which we denote as non-spherical (NS). Our US gold NPs feature near spherical forms and improved monodispersity both in shape and size. We demonstrate the first optical manipulation of US gold NPs in a near infrared optical trap both in liquid and air and report a trap stiffness with a 2-10 times lower standard deviation, compared to conventional NS gold NPs. This study highlights the exceptional sensitivity of the trapping parameters of gold NPs to their morphology. Trapped US particles may offer efficient handles for manipulation of biological molecules[13] as well as new studies of surface enhanced Raman scattering (SERS) and trapping where there is a desire to achieve sphericity.[14] Importantly our work also paves the way for controlled studies of optical binding, plasmon mediated light-matter interactions, and novel applications in optomechanics such as precise optical probing of weak forces and torques.

II. METHODS

A. Ultrasmooth gold nanoparticle synthesis

Our fabrication method is based on a growth followed by chemical etching process.[12] In the slow growth phase, monocrystalline polyhedral shapes are formed; edges and vertices are then isotropically removed during the slow chemical etching process, creating ultrasmooth, highly spherical gold NPs. We found that the final outcome in terms of the nanoparticle size is affected by the initial growth phase, likely as a result of relatively small changes to the reaction temperature. Lower temperatures lead to a slower rate of reduction of the gold salt, producing larger polyhedral crystallites[15] and consequently larger ultrasmooth NPs after the etching step. We prepared US gold NPs of 50 nm and 100 nm in diameter.

In brief, solutions of poly(diallyldimethylammonium chloride) (0.4 mℓ, 20 wt. % in H_2O, average Mw 400 000–500 000, Sigma-Aldrich) and phosphoric acid (0.8 mℓ, 1M, Sigma-Aldrich) were added to a round-bottom flask containing ethylene glycol (20 mℓ, Sigma-Aldrich), and the resulting solution was stirred for 2 min at room temperature. An aqueous solution of chloroauric acid (0.02 mℓ, 0.5M, Sigma-Aldrich) was then added and the mixture was stirred for a further 15 min at room temperature. The reaction was then heated to approximately 180 °C–205 °C and stirring continued for 30 min. We were unable to precisely control the internal reaction temperature at such high values. However, it was observed that larger nanocrystals were produced from batches where the average temperature measured over this period was at the lower end of the target range. After cooling to room temperature, a further aliquot of chloroauric acid was added (0.005 mℓ, 0.5M) and stirring continued for 20 h. The solution was centrifuged at 14 636 × g rcf, 5 °C for 20 min, leading to precipitation of gold NPs. The colorless supernatant was then carefully discharged, and the residue was suspended in fresh ethanol and sonicated for 15 min. The centrifugation–redispersion cycle was repeated a further two times. We note that the reproducibility of the size and circularity is found to be within ±10% over different batches.

B. Trapping in liquid

A circularly polarized collimated laser beam (IPG Photonics, continuous-wave at 1070 nm wavelength) is focused by a high numerical aperture (NA) microscope objective (Nikon E Plan 100×, NA = 1.25 in oil) to trap single gold NPs in liquid. We prepare colloidal suspensions of US and

NS gold NPs in heavy water (with a concentration of $\sim 1 \times 10^8$ mℓ^{-1}) to minimize heating due to absorption by the surrounding medium. The suspension is enclosed in a miniature cylindrical chamber (diameter 10 mm, height 0.1 mm) formed by a vinyl spacer and two glass cover slips. Particles are trapped at an axial distance of 4–5 μm above the glass surface to avoid any proximity effects. The forward scattered light from the trapped particle is collected by a condenser lens (Mitutoyo Plan Apo, 50×, NA = 0.55) and is sent to a quadrant photodiode (QPD, First Sensor, QP50-6SD2) to measure the particle position and to confirm that only one particle is trapped during each measurement.[2]

Once a single particle is trapped, its position power spectrum $S(f)$ is fitted to a Lorentzian curve with the corner frequency f_c, which defines how fast the trapped particle can move in a viscous medium. This quantity is used to calculate the trap stiffness as $\kappa = \Gamma(T)\,(2\pi f_c)$, where $\Gamma(T) = 6\pi\mu(T)r$ is the Stokes drag (damping) coefficient with r being the particle radius and $\mu(T)$ being the viscosity of the surrounding medium of temperature T. We measure the lateral trap stiffness κ_x and κ_y for two orthogonal directions x and y perpendicular to the beam axis z. Over 25 different particles from each sample are characterized at a fixed optical power of 45 mW in the trapping plane.

C. Trapping in air

The same setup as in liquid trapping is used for air trapping except for a sample chamber. Gold NPs are delivered to the trap through the chamber with a baffle structure based upon the design reported by Jauffred *et al.*[9] Ethanol droplets (3–5 μm in diameter) containing gold NPs (with a concentration of $\sim 1 \times 10^8$ mℓ^{-1}) are blown into the chamber by a nebulizer (Omron, micro air U22) via a fine nozzle. While droplets travel through two parallel baffles (formed by optically transparent sheets of acetate) with coaxial holes, ethanol is evaporated, thus leaving airborne NPs around the trap site. We measure the average lateral trap stiffness κ_{xy} of individual US and NS gold NPs for a range of optical power levels up to 0.5 W. At least five different NPs are tested for each particle type and size to obtain reliable statistics.

III. RESULTS AND DISCUSSION

A. Particle characteristics

We synthesized two samples of US gold NPs with the nominal diameters of 50 nm and 100 nm (see Methods for details). Scanning electron microscope (SEM) images of about 200 particles from each sample are characterized and compared with images of a random selection of NS particles of the corresponding size. Figure 1 shows a representative collection of the SEM images. Size distribution and circularity of the imaged gold NPs are summarized in Table I, where the diameter is the major-axis length and circularity is defined as the ratio between the actual area of an object and the area expected from its maximum Feret's diameter. Circularity ranges from zero (for a line segment) to unity (for a perfect circle).

Based on our analysis, both the monodispersity and circularity of US particles offer an improvement upon NS particles. This result is comparable to that reported by Lee *et al.*[12] Importantly, the standard deviation from perfect circularity of the US particles shows a reduction by a factor ranging
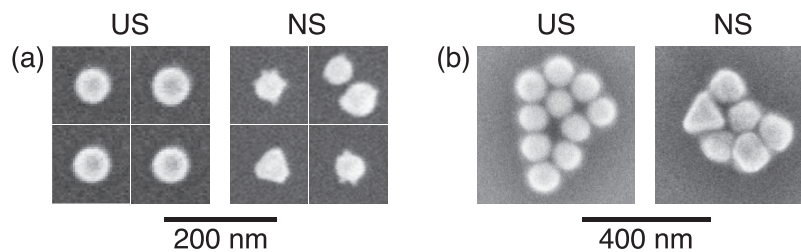

FIG. 1. Sample SEM (Hitachi S-4800, 30 kV) images of the gold NPs with the nominal diameter of (a) 50 nm and (b) 100 nm.

TABLE I. Physical parameters of gold NPs, where σ denotes the standard deviation.

Nominal diameter	50 nm		100 nm	
	US	NS	US	NS
Diameter (nm)	62.5	60.1	103.6	129.7
σ (nm)	5.4	6.6	8.6	13.1
Circularity (a.u.)	0.94	0.86	0.97	0.90
σ (a.u.)	0.03	0.08	0.01	0.12

between three and twelve compared to NS particles. This notable improvement in uniformity of shape can have a significant impact on the reproducibility of particle dynamics in an optical trap.

B. Trapping in liquid

Trap stiffness is a measure of the strength of an optical trap and the foundation of weak force measurement in an optical tweezers system (see Methods for details). Figure 2 shows the relation between κ_x and κ_y measured for different samples of gold NPs in liquid. The results are summarized in Table II, where κ_{xy} denotes the average lateral trap stiffness of κ_x and κ_y, and the measurement error is determined by the root mean square deviation $\sigma_{rms} = \sqrt{\Sigma(\kappa_x - \kappa_y)^2/N}$, where N is the number of measurements.

Notably, the stiffness of US gold NPs is lower (by 50–70%) than that of NS particles. This result is in agreement with the previous report that the particle morphology affects the trapping forces.[11] Importantly US NPs exhibit about a two-fold reduction in the measurement error (σ_{rms}) for stiffness (see Table II) compared to NS counterparts due to the improved circularity of US gold NPs (see Table I). We note that when trapped with a circularly polarized beam, one can expect laser-induced rotation of gold NPs,[16] in which case the stiffness is averaged over azimuth angles. Thus linearly polarized beam traps may result in more a pronounced difference in stiffness between US and NS gold NPs. We note that as discussed by Seol *et al.* and others, trap stiffness is subject to laser-induced heating of trapped gold NPs,[4,17–19] which is modeled using COMSOL and described
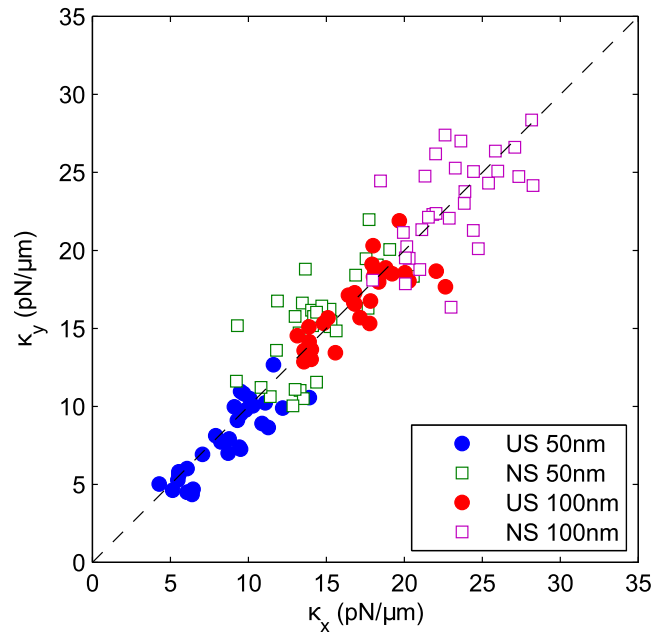

FIG. 2. Lateral trap stiffness κ_x and κ_y measured for gold NPs in liquid at a fixed optical power of 45 mW. The straight broken line has a gradient of unity.

TABLE II. Average lateral trap stiffness measured for gold NPs in liquid. All units are pNμm^{-1} W^{-1}.

Nominal diameter	50 nm		100 nm	
	US	NS	US	NS
κ_{xy}	8.21	14.83	16.70	22.92
σ_{rms}	1.40	2.52	1.42	2.68

later in this paper. As a result of the relatively low optical power of 45 mW in our case, the expected particle temperature rise (~10 °C for 100 nm gold NPs) should have but little effect on stiffness measurement.[4] However it would be intriguing to investigate how the shape of a gold NP influences its Brownian dynamics in an optical trap.

C. Trapping in air

The ability to manipulate individual metallic NPs in air or a vacuum can open up many exciting opportunities in levitated optomechanics, for example, the study of non-equilibrium Brownian dynamics at the nanoscale.[20,21] Recently, trapping of airborne NS gold NPs with diameters from 80 nm to 200 nm has been demonstrated.[9] This work has reported on trap stiffness measurements at a fixed optical power and has provided an initial estimate of the heating associated with particle absorption of the trapping beam. In our study, for the first time, we trap individual US and NS gold NPs (50 nm and 100 nm in diameter) in air for a range of optical power levels up to 0.5 W to reveal the effects of particle morphology.

The trap stiffness can be measured as $\kappa = \Gamma(T)\,(2\pi f_c)$, where $\Gamma(T) = 6\pi\mu(T)r$ if $\mu(T)$ is known (see Methods for details). It is possible to obtain a reliable data set of the temperature-dependent air viscosity but is limited to the range up to 600 K.[22] To avoid possible uncertainties in $\mu(T)$ for determining κ, we study the integral of the power spectral density (PSD) $S(f)$. This quantity is proportional to the mean square displacement of the particle $\langle\sigma^2\rangle$ and depends only upon trap stiffness κ and temperature T,[23,24]

$$\int_{-\infty}^{\infty} S(f)df = \langle\sigma^2\rangle = \frac{k_B T}{\kappa}, \tag{1}$$

where k_B is the Boltzmann constant. This is a well-established means of determining κ and T.[25] Figure 3 shows a series of position power spectra of an airborne US gold NP with a diameter of 100 nm trapped with a range of optical power from 0.1 W to 0.5 W. It is evident that the higher the power, the lower the integral of the PSD, which results in higher stiffness κ [see Eq. (1)]. It is noteworthy that the corner frequency f_c does not scale with the power P while $\kappa = \Gamma(T)\,(2\pi f_c) \propto P$. This is due to the fact that $\Gamma(T) \propto \mu(T)$ increases with T in air,[22] which gives rise to higher κ.
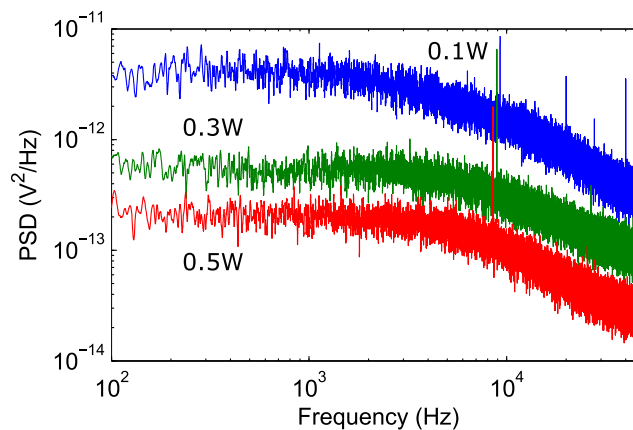

FIG. 3. Power spectra of an airborne US gold NP of 100 nm in diameter trapped with different optical power.

Once the QPD signal in volts (V) is calibrated by the particle position in meters (m),[26] the integration of $S(f)$ in units of $m^2\ Hz^{-1}$ over an infinite range of frequencies can be readily equated with the position variance in units of m^2. We note that Eq. (1) is only valid for systems in thermal equilibrium. For gold NPs with a diameter of 100 nm, the thermal equilibration time is 3.6 ns in water[4,27] and 90 ns in air, depending on their thermal conductivities (0.6 WmK^{-1} for water and 0.024 WmK^{-1} for air). These are both $>10^3$ times faster than the trapped particle motion with a corner frequency $f_c \leq 10$ kHz. Thus, the gold NPs trapped in water and in air follow the equipartition theorem and Eq. (1).

As the thermal conductivity of air is about 25 times lower than that of water, the temperature of air around a trapped gold NP is significantly higher than in water. We modeled the amount of energy absorbed by a gold NP positioned at the focus of the beam and the dissipation of the heat through conduction into air using the COMSOL Multiphysics software (RF module in scattering formulation).[10] The model calculates the absorption and scattering cross sections of a single airborne gold NP and estimates its temperature rise ΔT at a given incident power, which is 0.57 KmW^{-1} and 3.2 KmW^{-1} for particle diameters of 50 nm and 100 nm, respectively [see blue and green lines in Fig. 4(b)]. These predictions are in line with previous studies[4,9] where heating of trapped gold NPs is addressed using the same approximations (i.e., the dielectric function of gold NPs is stationary over elevated temperatures) as in this work. We use these calculated values of temperature together with the integral of the PSD $S(f)$ to determine the trap stiffness κ using Eq. (1).

Figure 4(a) shows the average lateral trap stiffness κ_{xy} of US (circles) and NS (squares) gold NPs as a function of optical power up to 0.5 W. The error bars indicate two standard deviations
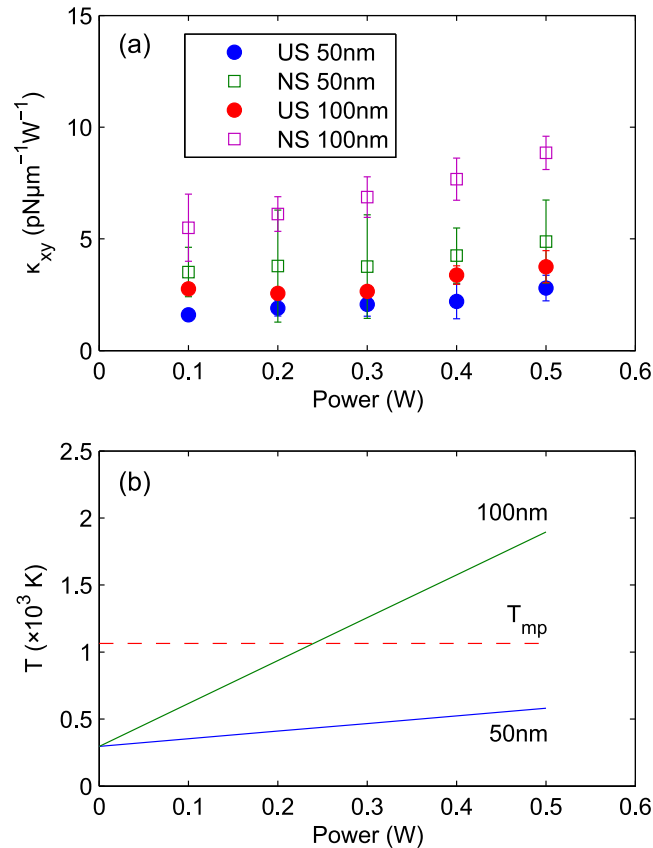

FIG. 4. Average lateral trap stiffness and particle temperature of airborne gold NPs. (a) Lateral stiffness measured for US (circles) and NS (squares) gold NPs of 50 nm and 100 nm in diameter. Error bars indicate $2\sigma_{xy}$. (b) Calculated particle temperature T of airborne gold NPs of 50 nm (blue) and 100 nm (green) in diameter. The horizontal line indicates the melting temperature $T_{mp} = 1064$ °C of gold.

TABLE III. Average lateral trap stiffness measured at 0.1 W for gold NPs trapped in air. All units are in pN μm^{-1} W^{-1}.

Particle diameter	50 nm		100 nm	
	US	NS	US	NS
κ_{xy}	1.60	3.51	2.76	5.50
σ_{xy}	0.28	1.11	0.15	1.50

($2\sigma_{xy}$) of the measurements for five different NPs. The stiffness of NS particles is about twice higher than that of US ones for both particle sizes (see Table III for summary), which agrees with the trend in liquid. Similarly, larger particles yield higher stiffness, which is also in an agreement with the previous study in air.[9] Importantly, the US particles exhibit a trap stiffness with a 4-10 times lower standard deviation, compared to the NS particles. We note that the stiffness of these gold NPs exhibits a superlinear dependence on optical power.

Figure 4(b) shows the calculated temperature T of gold NPs with diameters of 50 nm (blue) and 100 nm (green) for different optical power. Our model predicts $T \geq T_{mp} = 1064$ °C, exceeding the melting temperature of gold for the case of 100 nm. However, this temperature may be overestimated by the following reasons: Gold NPs can be trapped in regions where the optical power is significantly lower than in the focal plane. Off-maximum trapping is commonly observed in optical tweezers and verified in previous studies with gold nanoparticles.[28] The dielectric function of gold determines its optical properties and is highly temperature dependent, which changes the absorption cross section (σ_{abs}) and influences the resulting particle temperature depending on the wavelength under consideration.[29] At elevated temperatures, excited phonons will severely damp the electron oscillations, which reduces σ_{abs} of the gold NP. When trapped with increased optical power levels, the gold NPs will exhibit a much lower rate of temperature rise. The superlinearity of κ with respect to power found in Fig. 4(a) may indicate the overestimation of T due to the absence of determination of the temperature-dependent electron-phonon scattering rate. Further investigation is required to quantify σ_{abs}, which, however, is beyond the scope of the current study.

IV. CONCLUSIONS

In summary, we have synthesized US gold NPs of 50 nm and 100 nm in diameter and characterized their geometrical properties. Our US particles exhibit significantly improved circularity and monodispersity both in shape and in size compared to conventional NS particles of the corresponding size. We have demonstrated the first optical trapping of individual US gold NPs both in liquid and in air. Compared to conventional NS gold NPs, US particles exhibit approximately a two-fold reduction in standard deviation for trap stiffness measurements in liquid. Our data in air for the average lateral stiffness, at a fixed power of 0.1 W, show a reduction in standard deviation of stiffness by a factor between four and ten. Our study has revealed the exceptional sensitivity of the trapping parameters of gold NPs to their morphology. We have further demonstrated a more detailed understanding of thermal effects in the dynamics of optically trapped airborne gold NPs. US gold particles can pave the way for more controlled studies of SERS, plasmon mediated optical binding, spin angular momentum transfer[16,30] and may even perform as efficient handles for manipulation.[13] Furthermore, trapping of such US particles in air or a vacuum may open up new opportunities in levitated optomechanics.[9,25]

[1] K. Svoboda and S. M. Block, "Biological applications of optical forces," Annu. Rev. Biophys. Biomol. Struct. **23**, 247 (1994).

[2] P. M. Hansen, V. K. Bhatia, N. Harrit, and L. Oddershede, "Expanding the optical trapping range of gold nanoparticles," Nano Lett. **5**, 1937 (2005).

[3] J. J. Xiao, H. H. Zheng, Y. X. Sun, and Y. Yao, "Bipolar optical forces on dielectric and metallic nanoparticles by evanescent wave," Opt. Lett. **35**, 962 (2010).

[4] Y. Seol, A. E. Carpenter, and T. K. Perkins, "Gold nanoparticles: Enhanced optical trapping and sensitivity coupled with significant heating," Opt. Lett. **31**, 2429 (2006).

[5] A. Lehmuskero, P. Johansson, H. Rubinsztein-Dunlop, L. M. Tong, and M. Käll, "Laser trapping of colloidal metal nanoparticles," ACS Nano **9**, 3453 (2015).

[6] M. Dienerowitz, M. Mazilu, and K. Dholakia, "Optical manipulation of nanoparticles: A review," J. Nanophotonics **2**, 021875 (2008).

[7] M. Ploschner, T. Čižmár, M. Mazilu, A. Di Falco, and K. Dholakia, "Bidirectional optical sorting of gold nanoparticles," Nano Lett. **12**, 1923 (2012).

[8] V. Demergis and E.-L. Florin, "Ultrastrong optical binding of metallic nanoparticles," Nano Lett. **12**, 5756 (2012).

[9] L. Jauffred, S. M.-R. Taheri, R. Schmitt, H. Linke, and L. B. Oddershede, "Optical trapping of gold nanoparticles in air," Nano Lett. **15**, 4713 (2015).

[10] Y. Arita, M. Ploschner, M. Antkowiak, F. Gunn-Moore, and K. Dholakia, "Laser-induced breakdown of an optically trapped gold nanoparticle for single cell transfection," Opt. Lett. **38**, 3402 (2013).

[11] O. Brzobohatý, M. Šiler, J. Trojek, L. Chvátal, V. Karásek, and P. Zemánek, "Non-spherical gold nanoparticles trapped in optical tweezers: Shape matters," Opt. Express **23**, 8179 (2015).

[12] Y. J. Lee, N. B. Schade, L. Sun, J. A. Fan, D. R. Bae, M. M. Mariscal, G. Lee, F. Capasso, S. Sacanna, V. N. Manoharan, and G. R. Yi, "Ultrasmooth, highly spherical monocrystalline gold particles for precision plasmonics," ACS Nano **7**, 11064 (2013).

[13] T. T. Perkins, "Ångström-precision optical traps and applications," Annu. Rev. Biophys. **43**, 279 (2014).

[14] F. Benz, R. Chikkaraddy, A. Salmon, H. Ohadi, B. de Nijs, J. Mertens, C. Carnegie, R. W. Bowman, and J. J. Baumberg, "SERS of individual nanoparticles on a mirror: Size does matter, but so does shape," J. Phys. Chem. Lett. **7**, 2264–2269 (2016).

[15] C. Li, K. L. Shuford, M. Chen, E. J. Lee, and S. O. Cho, "A facile polyol route to uniform gold octahedra with tailorable size and their optical properties," ACS Nano **2**, 1760 (2008).

[16] A. Lehmuskero, R. Ogier, T. Gschneidtner, P. Johansson, and M. Käll, "Ultrafast spinning of gold nanoparticles in water using circularly polarized light," Nano Lett. **13**, 3129 (2013).

[17] D. Rings, R. Schachoff, M. Selmke, F. Cichos, and K. Kroy, "Hot Brownian motion," Phys. Rev. Lett. **105**, 090604 (2010).

[18] D. Rings, D. Chakraborty, and K. Kroy, "Rotational hot Brownian motion," New J. Phys. **14**, 053012 (2012).

[19] Y. Arita, J. M. Richards, M. Mazilu, G. C. Spalding, S. E. S. Spesyvtseva, D. Craig, and K. Dholakia, "Rotational dynamics and heating of trapped nanovaterite particles," ACS Nano **10**, 11505 (2016).

[20] J. Millen, T. Deesuwan, P. Barker, and J. Anders, "Nanoscale temperature measurements using non-equilibrium Brownian dynamics of a levitated nanosphere," Nat. Nanotechnol. **9**, 425 (2014).

[21] K. Kroy, "Levitating nanoparticles non-equilibrium nano-thermometry," Nat. Nanotechnol. **9**, 415 (2014).

[22] G. W. C. Kaye and T. H. Laby, *Tables of Physical and Chemical Constants*, 16th ed. (Longman, London, 1995).

[23] P. F. Cohadon, A. Heidmann, and M. Pinard, "Cooling of a mirror by radiation pressure," Phys. Rev. Lett. **83**, 3174–3177 (1999).

[24] D. Kleckner and D. Bouwmeester, "Sub-kelvin optical cooling of a micromechanical resonator," Nature **444**, 75–78 (2006).

[25] Y. Arita, M. Mazilu, and K. Dholakia, "Laser-induced rotation and cooling of a trapped microgyroscope in vacuum," Nat. Commun. **4**, 2374 (2013).

[26] W. M. Lee, P. J. Reece, R. F. Marchington, N. K. Metzger, and K. Dholakia, "Construction and calibration of an optical trap on a fluorescence optical microscope," Nat. Protoc. **2**, 3226–3238 (2007).

[27] V. K. Pustovalov, "Thermal-processes under the action of laser-radiation pulse on absorbing granules in heterogeneous biotissues," Int. J. Heat Mass Transfer **36**, 391–399 (1993).

[28] A. Kyrsting, P. M. Bendix, D. G. Stamou, and L. B. Oddershede, "Heat profiling of three-dimensionally optically trapped gold nanoparticles using vesicle cargo release," Nano Lett. **11**, 888–892 (2011).

[29] O. A. Yeshchenko, I. S. Bondarchuk, V. S. Gurin, I. M. Dmitruk, and A. V. Kotko, "Temperature dependence of the surface plasmon resonance in gold nanoparticles," Surf. Sci. **608**, 275–281 (2013).

[30] L. Shao, Z.-J. Yang, D. Andrén, P. Johansson, and M. Käll, "Gold nanorod rotary motors driven by resonant light scattering," ACS Nano **9**, 12542 (2015).